Cerebral Cortex, 2021, 1–16
https://doi.org/10.1093/cercor/bhab425
Original Article

It's in the Timing: Reduced Temporal Precision in Neural Activity of Schizophrenia

Annemarie Wolff[1], Javier Gomez-Pilar[2,3], Jianfeng Zhang[4,5], Joelle Choueiry[1], Sara de la Salle[1], Verner Knott[1] and Georg Northoff[1,6]

[1]University of Ottawa Institute of Mental Health Research, Ottawa, ON K1Z 7K4, Canada
[2]Biomedical Engineering Group, Higher Technical School of Telecommunications Engineering, University of Valladolid, Valladolid 47011, Spain
[3]Centro de Investigación Biomédica en Red—Bioingeniería, Biomateriales y Nanomedicina (CIBER-BBN), Madrid 28029, Spain
[4]Mental Health Center, Zhejiang University School of Medicine, Hangzhou 310058, China
[5]College of Biomedical Engineering and Instrument Sciences, Zhejiang University, Hangzhou 310027, China
[6]Brain and Mind Research Institute, University of Ottawa, Ottawa, ON K1Z 7K4, Canada
Address correspondence to Annemarie Wolff, 1145 Carling Avenue, room 6433 Ottawa, ON K1Z 7K4. Email: awolf037@uottawa.ca

Abstract

Studies of perception and cognition in schizophrenia (SCZ) show neuronal background noise (ongoing activity) to intermittently overwhelm the processing of external stimuli. This increased noise, relative to the activity evoked by the stimulus, results in temporal imprecision and higher variability of behavioral responses. What, however, are the neural correlates of temporal imprecision in SCZ behavior? We first report a decrease in electroencephalography signal-to-noise ratio (SNR) in two SCZ datasets and tasks in the broadband (1–80 Hz), theta (4–8 Hz), and alpha (8–13 Hz) bands. SCZ participants also show lower inter-trial phase coherence (ITPC)—consistency over trials in the phase of the signal—in theta. From these ITPC results, we varied phase offsets in a computational simulation, which illustrated phase-based temporal desynchronization. This modeling also provided a necessary link to our results and showed decreased neural synchrony in SCZ in both datasets and tasks when compared with healthy controls. Finally, we showed that reduced SNR and ITPC are related and showed a relationship to temporal precision on the behavioral level, namely reaction times. In conclusion, we demonstrate how temporal imprecision in SCZ neural activity—reduced relative signal strength and phase coherence—mediates temporal imprecision on the behavioral level.

Keywords: electroencephalography, inter-trial phase coherence, schizophrenia, signal-to-noise ratio, synchrony, temporal precision

Introduction

Imagine you are having a conversation with a friend in a large room, surrounded by others engaged in similar conversations. Your friend's voice is intermittently drowned out by the ongoing chatter of the background noise, which rises and falls. This makes it possible for you to hear only parts of what they are saying. Your friend asks you questions, but you respond to only some of them; you can't hear the others because of the relative noise in the room.

That, as several studies on sensory perception (Javitt 2009; Sass et al. 2013; Vlcek et al. 2014; Javitt and Freedman 2015; Micoulaud-Franchi et al. 2016; Hoptman et al. 2018) and cognition (Schwartz et al. 1989; Birkett et al. 2007) suggest, may be the situation for someone with schizophrenia (SCZ). Specifically, their brain's neuronal background activity (here the ongoing spontaneous activity is considered to be noise) may intermittently overwhelm the processing of external stimuli (here the stimulus-evoked (David et al. 2006) activity is considered to be signal) from the environment (Yang et al. 2014, 2017); increased background noise (Yang et al. 2014, 2017) has previously been shown. The ratio of these two factors, as measured by the signal-to-noise ratio (SNR), would be lower as a result, which has shown to be the case in SCZ (Winterer et al. 1999, 2000; Winterer and Weinberger 2004). This neuronal background activity intermittently drowning out the stimulus—as measured by the SNR (Xia 1998)—hampers the consistency, or temporal precision (hereafter termed temporal precision), in the processing of external stimuli or tasks (Andreasen et al. 1999; Thoenes and Oberfeld 2017) in SCZ participants. As in our example above, the problem in SCZ may not be one of accuracy—incorrectly hearing the words—but lack of precision due to variability in perceiving and responding to the stimuli (Thoenes and Oberfeld 2017).

Supported by several studies (Andreasen et al. 1999; Thoenes and Oberfeld 2017) and reinforced by functional and anatomical evidence (Andreasen and Pierson 2008), a long-held theory of cognitive processing deficits in SCZ is that there is (Winterer and Weinberger 2004) mistiming of information processing at the neural encoding (action potential) level, which leads to deficits in performance and behavior (Andreasen et al. 1999). This theory is supported by findings that SCZ participants show the same accuracy in their behavior—correct responses to a stimulus—as healthy controls, but significantly lower temporal precision—greater variability of the responses to

Received: August 10, 2021. **Revised:** October 29, 2021. **Accepted:** November 2, 2021

the same stimulus upon repeated presentations including an impairment in synchrony (Andreasen et al. 1999; Thoenes and Oberfeld 2017). For example, a recent meta-analysis showed no significant effect between patients and controls over all tasks in accuracy of time perception (Bolbecker et al. 2014; Thoenes and Oberfeld 2017). A large effect across all time perception tasks was found, however, in precision in patients with SCZ. They found that the deviation from the true time in the time perception tasks was the same in SCZ as healthy controls, but the SCZ participants' responses varied significantly more. What is unclear, however, are the neural correlates of such temporal imprecision on a behavioral level.

To address this, the goal of our study is to investigate temporal precision in SCZ on a neural level, linking it to temporal precision in behavior. Since precision is the inverse of variance, high variance (low coherence) in neural activity over trials is equivalent to low precision or imprecision. Is the neuronal activity in SCZ by itself less regular and consistent, and consequently less temporally precise in its neural processing of external stimuli? And if so, what is the underlying mechanism and how does it impact behavior? The answers to these two questions are unclear. Addressing them is of key importance for determining what underlies temporally imprecise behavior in SCZ (Kesby et al. 2018; Weele et al. 2019; Abi-Dargham 2020; Frankle and Narendran 2020).

If there is a difference in temporal precision of the neural activity over trials in SCZ, then we would expect this to be present in all sensory modalities and tasks. We therefore investigated two different SCZ data sets (including healthy controls) in electroencephalography (EEG) with different task states and sensory modalities to determine if this finding was wide-ranging or specific only to one type of task or modality. Aimed at probing temporal precision on the neural level, we used SNR and inter-trial phase coherence (ITPC) measures as evidence to support temporal precision. SNR measures the ratio of the stimulus evoked activity to the ongoing spontaneous activity over trials, while ITPC measures the consistency of the phase of the signal over all trials. Low phase consistency over trials (high variance) would lead to low ITPC so low precision—imprecision—of phase over trials.

First, we investigated the SNR in a dynamic way, that is, in its time course (rather than in a static way as in two earlier SNR studies; Winterer et al. 1999, 2000). Such a dynamic approach makes it possible to link the SNR with temporal regularity and precision in the neural processing of an external stimulus. Building on and extending the earlier findings (Winterer et al. 1999, 2000), we hypothesized that a reduced SNR in SCZ participants, in theta specifically, is related to decreased temporal synchronization compared with healthy subjects. The theta frequency band (4–8 Hz) is known to have a role in cognitive functions (Korotkova et al. 2018) such as spatial coding (Hafting et al. 2008), memory formation (Berry and Thompson 1978), and anxiety-specific behaviors (Gray 1982). Prominent across species (Korotkova et al. 2018), theta has also shown significant differences in schizophrenic patients (decreased inter-trial coherence and event-related spectral perturbation) when compared with healthy controls (Csukly et al. 2014; Gomez-Pilar et al. 2018; Javitt et al. 2018; Hamilton et al. 2020; Roach et al. 2021).

Secondly, we investigated phase coherence over trials using ITPC. From these ITPC results, we inferred that the differences seen between groups were a result of varying phase offsets across trials when the ITPC was computed. This was supported mathematically by the equation for ITPC (equation 4); however, the degree of phase offsets was unknown. Employing computational simulation (Einevoll et al. 2019; Fan and Markram 2019), we validated the underlying mechanism of our findings. As our results measured the ITPC over all trials and inferred down what the constituents of each individual trial were, our computational modeling did the reverse: We simulated each trial with the components of the signal and the varying of the independent variable (phase offsets) and then measured the ITPC up at the level of all trials. The results from both—the measurement of ITPC—were finally compared. This linked our results to this modeling which showed a relation to temporal synchronization of neural activity relative to the timing of stimulus onset. We hypothesize reduced ITPC, again specifically in theta (Csukly et al. 2014; Gomez-Pilar et al. 2018; Javitt et al. 2018; Roach et al. 2021), in SCZ as being related to decreased temporal synchronization.

Finally, we link SNR and ITPC with each other, as well as to timing on the behavioral level, that is, reaction times. We expect reductions in theta and alpha SNR and theta ITPC to be interrelated (based on their commonly shared temporal imprecision), which also should impact temporal precision of reaction times on the behavioral level.

Materials and Methods

As we hypothesized that participants with SCZ have weaker stimulus-related signal relative to the background noise resulting in a lower SNR, this relatively weak signal would be universal and consistent across all sensory modalities (visual, auditory, etc.) and all experimental paradigms (perceptual, cognitive, sensory, etc.). For this reason, we analyzed two separate SCZ datasets with different experimental paradigms (cognitive cost conflict, sensory P50) and sensory modalities (visual, auditory). In addition, one was a report paradigm (i.e., respond with a button press) and one was no report (no response) (Tsuchiya et al. 2015). Moreover, as to minimize effects of prediction (Lakatos et al. 2013; Rentzsch et al. 2015; Sterzer et al. 2018; Albrecht et al. 2019), stimuli were presented in a temporally irregular way in these paradigms, that is, jittered, with variable inter-trial intervals (ITIs).

Table 1. Dataset specifications

Label	Mod.	Type	Report	Associated Publications
Dataset 1	Vis.	Cog.	Y	Albrecht MA, et al. 2019. Increased conflict-induced slowing, but no differences in conflict-induced positive or negative prediction error learning in patients with schizophrenia. Neuropsychologia. 123(di):131–40.
Dataset 2	Aud.	Sen.	N	Choueiry J, et al. 2019. Combining CDP-choline and galantamine, an optimized $\alpha 7$ nicotinic strategy, to ameliorate sensory gating to speech stimuli in schizophrenia. Int J Psychophysiol. 145(February):70–82.

Note: Vis., visual; Aud., auditory; Cog., cognitive; Sen., sensory; Y, yes; N, no.

Table 2. Number of trials in analyzed datasets

Dataset	Number of trials
Dataset 1	216
Dataset 2	50

Datasets

In this study, two separate datasets were analyzed (Table 1). One dataset involved analyzing stimuli from a visual cognitive task with a response (first dataset), while the other dataset was composed of analyzing stimuli from an auditory perceptual task with no response (second dataset). Therefore, there were differences for the two datasets for modality (visual, auditory), type (cognitive, sensory), and response (response, no response) (Table 1). We chose this approach to determine how generalizable our results were. As per our hypothesis, the difference in SNR should be true for all tasks, senses, and paradigms. For that reason, we chose these two sensory modalities and types of stimuli.

Finally, the dataset with the response allowed us to use the reaction times to investigate the behavioral significance of SNR and ITPC. The dataset without a response (no-report) allowed us to look at differences without any data contamination related to the motor or cognitive aspects of a behavioral response (Tsuchiya et al. 2015).

Once all the EEG data were preprocessed for each dataset, the number of all trials per participant was calculated. The participant with the lowest number of trials determined the total number analyzed in each participant; that number of trials was then randomly selected in each participant. Therefore, the data analyzed for each participant in each dataset were based on the same number of trials (Table 2).

For both datasets, as detailed in each of the associated publications (Table 1), all participants provided written informed consent prior to participation in each respective study. All study protocols were completed according to the ethics guidelines of each respective research institution. In addition, for the use of these datasets in this study after all participants provided informed consent for the original studies, research ethics board approval was obtained (REB-2021002) at the University of Ottawa's Institute of Mental Health research, the home institute of the first and last author.

SCZ Dataset 1

The EEG data for the first dataset (hereafter titled "Dataset 1") (Albrecht et al. 2019) were obtained from the Patient Repository for EEG Data + Computational Tools (PREDICT) data repository located at *predict.cs.unm.edu*. Dataset 1 comprised EEG task data from 44 schizophrenic patients (22 medicated with clozapine, 22 medicated with a second generation antipsychotic) and 31 healthy controls (Supplementary Table 1). EEG data were recorded with 64 channels using a Brain Vision cap and amplifier system (Brain Vision Gmbh). Details can be seen at the dataset's associated published paper (Albrecht et al. 2019).

The task consisted of a visual cognitive Cost Conflict task. There was a training and testing phase of the task, though only training trials were analyzed in this study. During each trial, one of four unique simple shapes (star, oval, rectangle, hexagon) in color (blue, yellow) was presented. They were told to respond by pressing a button (left, right) to get a reward of 1 point (+1) within a response window of 850 ms. Incorrect responses resulted in no reward (0)—zero points awarded—and responses beyond the 850 ms response window were punished by removal of three points (−3). Only the first 500 ms after stimulus onset (0–500 ms) were analyzed in this study.

Of the four stimuli, one (A) was rewarded at a rate of 100% regardless of which button the participant pressed (left, right); they were always awarded +1. The second stimulus (D) was rewarded at a rate of 0% regardless of which button the participant pressed; they were always rewarded +0. The two remaining stimuli were reinforced at 50% on average, but this depended on the conflict (congruent, incongruent). Stimulus B was reinforced at a rate of 100% on congruent trials and 0% on incongruent, while the opposite was true for stimulus C (0% for congruent, 100% for incongruent).

Participants completed four blocks of trials and each block contained at least 20 correct responses for each stimulus. In the training phase, the block order was as follows: 1) the ITI was a fixation cross presented for 1000 ms; 2) the stimulus was presented until they responded or for a maximum of 850 ms; 3) a short 170 ms fixation cross (±10 ms, jittered); 4) feedback (+1, 0, −3) was presented for 1000 ms. In the testing phase, the feedback was not provided.

For the analysis, only the training trials were used as the behavioral data (reaction times) were better for them

than for the test data. Once all the EEG data were preprocessed, the number of all training trials per participant was calculated. The participant with the lowest number of trials determined the total number analyzed in each participant as that number of trials was then randomly selected in each participant. Therefore, the data analyzed for each participant were based on the same number of training trials.

SCZ Dataset 2

The second dataset (hereafter titled "Dataset 2") (Choueiry et al. 2019) consisted of 26 participants with a clinical diagnosis of SCZ according to DSM-IV criteria, and 25 healthy controls (Supplementary Table 1). SCZ participants were clinically stable for at least 3 months and had been on a stable antipsychotic regimen for at least 4 weeks at the time of participation (for further details of participants, please see Supplementary Materials). Exclusion criteria were diagnosis of other medical illness, treatment with clozapine, head injury with loss of consciousness in past 6 months, and hearing impairment. Of the 26 participants, 16 were smokers and 8 nonsmokers (<100 smoked cigarettes in lifetime, zero tobacco product consumption in preceding year). Study procedures and participant recruitment were done in compliance with the Research Ethics Board of The Royal Ottawa Mental Health Care Group and the University of Ottawa.

The EEG recording was done using a Brain Vision (Brain Products, Gmbh, Munich, Germany) 30 electrode EasyCap, software (Recorder) and amplifier (Quickamp). The electrodes were placed according to the 10/20 international system (Jurcak et al. 2007) with additional electrodes placed around the eye (above/below, left/right) to record vertical and horizontal ocular activity. The online reference was placed between FPz and Fz and the electrode impedance was kept below 5 kΩ throughout the recording session.

Participants were presented a P50 paradigm, though only the first of the paired stimuli were analyzed in this study (S_1 of an S_1–S_2 pairing). The stimulus was an "a" vowel (170 ms long, 140 Hz) presented binaurally through headphones at 80 dB (SPL). The two stimuli were presented with 500 ms between them. Therefore, only the first 500 ms of the trial was analyzed to remove any influence of the second stimulus.

In this study, two identical P50 paradigm and EEG recording sessions were completed by each participant, one after the administration of a placebo and the other after the administration of cytidine diphosphocholine (CDP-choline) and galantamine. The order of the sessions was counterbalanced. Only the EEG data from the placebo session were analyzed in this study; thus, there was no effect of a pharmacological agent.

EEG Preprocessing

All EEG data preprocessing was completed using EEGLAB (v2019) (Delorme and Makeig 2004), which required MATLAB (The MathWorks) v2018a, including the use of the Optimization, Statistics, and Signal Processing Toolboxes. To ensure that our finding with the SNR was due to neuronal noise only and not any artifacts from the hardware or recording of the EEG data, we employed a rigorous preprocessing regime to remove as many artifacts from the EEG data as possible prior to beginning analysis (see Supplementary Table 2 for details).

Raw EEG data were imported to EEGLAB and were resampled to 500 Hz (if the raw data had a sampling rate of 1000 Hz) using their anti-aliasing *resample* function. The continuous data were then low- and high-pass FIR filtered from 1 to 80 Hz. The data were then visually inspected. Flat electrode channels were removed if they were flat longer than 5 s (see Supplementary Table 2 for the numbers of all artifacts removed). Next, noisy channels were removed if they had the following properties: correlation of mean over 5 s of less than 0.85 with other channels (Bigdely-Shamlo et al. 2015); mean value over 5 s greater than 4 standard deviations (SD) from the mean of all channels. The EEG data were then rereferenced to the average activity of all channels, and the removed channels were spherically interpolated. Cleanline (Mullen 2012) at 60 Hz was then used to remove line noise. The parameters were sliding window length and step of 4 s (no overlap), default smoothing factor of 100, default *P* value of 0.01 for detecting significant sinusoid, and an FFT default padding factor of 2.

The continuous data were then epoched from 800 ms before stimulus onset to 1100 ms after stimulus onset, with no baseline correction. All stationary artifacts, specifically eye movements, were reduced using independent component analysis and the Multiple Artifact Rejection Algorithm (Winkler et al. 2011, 2014). After the removal of these final artifacts, the EEG data were rereferenced to the surface Laplacian (Carvalhaes and De Barros 2015), a spatial filter, in order to allow for greater spatial specificity of the data.

Event-Related Potentials and Electrode Choice with Topoplots

Before plotting the event-related potentials (ERPs), the epochs in the data were baseline corrected with a baseline of 400 ms before stimulus onset to stimulus onset (−400 to 0 ms). ERPs were the mean of trials for all stimuli for each dataset (Table 2) and each electrode. After visualizing the data with a butterfly plot (Supplementary Fig. 1a) for all electrodes, one early (<200 ms) interval of 40 ms was chosen for the topoplots (Supplementary Fig. 1b). This interval was 116–156 ms for Dataset 1 and 88–128 ms for Dataset 2.

We first made butterfly plots that visualized the mean of all trials for each electrode (Supplementary Fig. 1a). An early (<250 ms) 40 ms time interval in which the activity of all individual electrodes diverges was chosen for visualization in the topoplots based on these butterfly plots. The mean ERP activity of this time interval (116–156 ms for Dataset 1, 88–128 ms for Dataset 2) for all

electrodes was then calculated and plotted as topoplots (Supplementary Fig. 1b). From these topoplots, but also from previous studies (Csukly et al. 2014; Hamilton et al. 2020; Roach et al. 2021) which found significant deficits in SCZ in the theta band (maximal in the frontal region), two electrodes were chosen in each data set. One in the primary sensory cortices (PO8 for visual paradigm and Cz for auditory paradigm respectively), and one in the frontal cortex (AFp9 and Fp1 respectively) as our hypothesis specified a significant difference in the theta band, and this frequency band is maximal in the frontal region. The electrode in the primary sensory cortices was chosen as this was early sensory activity, while the electrode in the frontal cortex was chosen as a result of previous SCZ findings (Egan et al. 2001; Weinberger et al. 2001; Winterer and Weinberger 2004; Rolls et al. 2008; Csukly et al. 2014; Weele et al. 2019) in frontal cortical activity, and as our hypotheses centered on frontal theta activity specifically. ERPs were plotted for these two electrodes and the area under the curve (AUC) was calculated and statistically compared.

Based on visual inspection of the topoplots and previous SCZ results found in the frontal cortex (Egan et al. 2001; Weinberger et al. 2001; Winterer and Weinberger 2004; Rolls et al. 2008; Csukly et al. 2014; Weele et al. 2019), and as done in a previous study (Arazi et al. 2017), two electrodes were chosen from the frontal cortex and the sensory cortices. The ERPs for these two electrodes were plotted and the AUC for the ERPs in the same interval was calculated (Supplementary Fig. 1c). All subsequent analyses were done with the specified electrode from the frontal cortex (AFp9 for Dataset 1, Fp1 for Dataset 2).

SNR and Cross-correlation Delay Analysis

SNR was calculated according to the methods of Xia (1998). As we wanted to have a time-resolved SNR measure, instead of taking the mean over the full time interval of interest (0–500 ms), it was measured at each timepoint between stimulus onset and 500 ms. The interval of interest was 500 ms as the stimulus in the second dataset was a paired P50 auditory stimulus, with 500 ms between tones. The second tone was presented 500 ms after stimulus onset of the first tone; we only analyzed data from the first tone in this study.

Specifically, signal was calculated as

$$X_i = \left(t_i - \langle b \rangle\right)^2 \tag{1}$$

where $t_i$is the mean value over trials at timepoint i between stimulus onset (0 ms) and 500 ms and $\langle b \rangle$ is the mean of the mean baseline over trials from −400 ms to stimulus onset. The noise was then calculated as

$$\eta_i = (t_i)^2 \tag{2}$$

where $t_i$is the mean value over trials at timepoint i between stimulus onset and 500 ms. Finally, the SNR was the ratio of the two, converted to decibels

$$\Phi_i = 10 \times \log_{10}\left(\frac{X_i}{\eta_i}\right) \tag{3}$$

Finally, the mean of the SNR was calculated in a sliding window. The window length was 76 ms with a 50% overlap.

To verify that our results were not due to length of sliding window or the size of the overlap, we did the same analysis with an additional window length (100 ms) and overlap (90%) (Supplementary Fig. 2). We found the same results as described above. In addition, we measured the SNR AUC in the later time interval with the same window length and overlap to see if our significant results were in both time intervals (Supplementary Fig. 3). We did not find significant differences in the later time interval; therefore, our significant findings in the AUC of the SNR curves are confined to the early time interval and are not due to our choice of window length or overlap.

Inter-trial Phase Coherence

ITPC was computed using complex Morlet wavelets according to:

$$\mathrm{ITPC_{tf}} = \left| n^{-1} \sum_{r=1}^{n} e^{\mathrm{i}k_{tfr}} \right|, \tag{4}$$

where n is the number of trials, r is the trial number, e^{ik} is Euler's formula providing the complex polar representation of a phase angle k on trial r at time-frequency point tf, and the absolute value bars indicate the length of the average vector. Complex Morlet wavelets were computed for the full epoch length (−800 to 1100 ms) between 1 and 80 Hz. The wavelets were composed of 3–10 logarithmically spaced cycles and 158 points in the frequency range (80 – 1 Hz is 79 Hz, and two points per Hz = 158 points).

A recent paper (Van Diepen and Mazaheri 2018) used simulations to show that differences in amplitude and/or power can affect the measure of phase, specifically in ITPC. They showed that lower amplitude leads to lower values of ITPC even though amplitude and phase are mathematically independent. We found differences in ERPs between groups in our data. ERPs, however, are baseline corrected while the trials with which ITPC is calculated are not. We therefore did a secondary analysis to determine if the median and standard deviation (SD) of the amplitude (0–500 ms) of the non-baseline corrected data—used to calculate the ITPC—differed between groups. For all datasets and groups, Mann–Whitney U tests found no significant difference in median or SD of amplitude between the SCZ participants and the healthy controls (Supplementary Table 4 for statistics). Therefore, the differences found in ITPC between the groups were not due to differences in amplitude.

ITPC Simulations

The ITPC simulations were based on a simple sine wave, which would replicate the ERSP results common to both groups and datasets. As this increase in theta power lasted only several hundreds of milliseconds (was not continuous), we decided that our simulations would have a transient oscillation with peaks in the theta range of 4–8 Hz (Supplementary Fig. 5b, far left plot). The base sine wave is

$$\sim_{\text{base}} = A \sin\left(2\pi f t + \Delta\theta r\right), \tag{5}$$

where A is the amplitude of the wave (here equal to 1), f is the frequency of the transient oscillation (4–8 Hz in increments of 1 Hz), and t is the timepoint in the trial. $\Delta\theta$ is the phase shift, which is the independent factor being varied in these simulations. The phase shifts ranged from 0 (no phase shift) to 2π (complete phase shift) with five levels ($0, \pi/2, \pi, 3\pi/2, 2\pi$). Finally, r, which is multiplied by the phase shift, is a number between 0 and 1, which is randomly generated for each trial. This creates some differences between trials for each phase shift.

For a transient oscillation, a Gaussian kernel in the time domain is applied to the sine wave, thereby allowing for the sine wave during a specified time window rather than continuously. The Gaussian kernel (Γ) is defined as

$$\Gamma = e^{\frac{-(t-p)^2}{2s^2}} \tag{6}$$

Where t is the timepoint, p is the peak time of the Gaussian kernel, and s is its width. In our simulations, the Gaussian kernel had a peak at 175 ms after stimulus onset and a full-width at half-maximum (FWHM) of 150 ms (Supplementary Fig. 5b, middle left plot). It was applied to the sine wave, and so the combination of these two components results in a transient increase of theta power after stimulus onset like that seen in the ERSP results of our actual data (Supplementary Figs 5a and 7).

Finally, we added two types of noise to the sine wave in order to make the simulations more realistic: 1) pink noise, which has a $\frac{1}{f}$ power spectrum (Supplementary Fig. 5b, far right plot) with an exponential decay of 50; 2) white noise, which has a flat power spectrum (Baker and Richard 2019; Guevara Erra et al. 2019; Qu et al. 2019; Aghababaiyan 2020).

To determine which of the phase-shifted simulations had the closest ITPC distance to the actual data, the Euclidean distance (d^2) was measured as

$$d^2_{\text{as}} = \left(x_a - y_s\right)\left(x_a - y_s\right)' \tag{7}$$

where x_a is the vector of the actual ITPC and y_s is the vector of the simulated ITPC. The simulation with the smallest value of d^2 was considered to be the simulation closest to the actual data.

To approximate Dataset 1, 38 (mean of 31 CON and 44 SCZ) single channels (one channel represents one participant) and 216 trials were simulated. For Dataset 2, 26 participants with one channel each and 50 trials were simulated. The mean ITPC of all trials and participants was then done (Fig. 5*d*). The mean ERSP was also calculated to verify the transient increase in theta power after stimulus onset (see Supplementary Fig. 7).

Reaction Times and Correlations

The behavioral relevance of SNR was examined by splitting the trials according to their reaction times. For each participant, all trials were ordered according to the reaction time of the response in each trial. The fastest and slowest 40% of trials were then chosen, and from these trials, the SNR was calculated. The middle 20% of trials according to reaction time were discarded. This resulted in one SNR curve for fast trials and one for slow trials for each participant. The AUC of the curve in the same time intervals was then calculated and compared statistically. The ITPC of the fast and slow trials was also calculated, and the results for each participant from 150–400 ms and 1–2.5 Hz were extracted and statistically compared.

The correlations were Spearman two-tail correlations, and the model fit was a linear model (polynomial 1) using MATLAB function *fit*. To take a dimensional approach, we did this across all participants without separating them into groups. To ensure, however, that our significant correlations were not due to the statistical differences between the two groups, we also correlated the variables separately for each group (Supplementary Fig. 9). This showed that our significant correlations were not a result of the differences between SCZ and CON.

Multiple Linear Regression Analyses

To determine if ITPC and SNR AUC predicted reaction times, a multiple linear regression in each experimental group was conducted. After preprocessing of the data, the participant with the lowest number of trials was 216. So that all participants had this same number, the regression analysis randomly selected 216 trials for each participant. The reaction times of these randomly selected trials were sorted and divided into three intervals (72 trials each). The slowest 72 trials were thus grouped together and the mean reaction time calculated, and the corresponding EEG data from these trials were likewise grouped. The same occurred for the other two intervals. From these EEG data in each interval, the ITPC and SNR were computed (at electrode AFp1). The data for each grouping, and for each participant, between stimulus onset (0 ms) and 200 ms were extracted, and between 1 and 8 Hz for the ITPC. These intervals were chosen as it was this range of time and frequencies where our previous results had been found. The mean of this time (and frequency interval) was then computed. This produced three values—one for each interval—for each participant and for each measure.

As these measures are computed over trials, a linear regression at the level of each individual participant was not feasible. The values for each experimental group were therefore combined. For each linear regression, one participant had three datapoints, one for each reaction time interval (slowest, middle, fastest).

The multiple linear regression was computed in MATLAB using function *fitlm*. The predictors were the ITPC AUC and the SNR AUC. The response (predicted variable) was the mean reaction time.

Statistics

Statistical testing between the healthy control group and the experimental group for each measure was done via the nonparametric Mann–Whitney *U* test. The reason for this was that the results were not normally distributed and were independent (healthy controls, experimental group).

To control for multiple statistical tests, the false discovery rate (Benjamini and Hochberg 1995) was applied to all statistical tests. Therefore, all *P* values reported below have been corrected for multiple comparisons.

Results

Early SNR and ITPC Is Lower in SCZ, with Longer Temporal Delays between SNR Signals in the Theta and Alpha Bands

We started our analysis by computing ERPs in all electrodes (64 in Dataset 1, 32 in Dataset 2) according to a recent publication (Arazi et al. 2017) (Supplementary Fig. 1). Based on the butterfly charts and topoplots, we selected the time intervals and electrodes (one in the frontal area, one in the primary sensory area, so occipital for Dataset 1 and central for Dataset 2) (see Arazi et al. 2017 for similar methods, see Methods section for details, and see Supplementary Fig. 1 for locations). The AUC was significantly different in SCZ compared with healthy controls in both datasets (Dataset 1: $Z_{frontal} = 2.082$ and $p_{frontal} = 0.037$, $Z_{occipital} = 2.426$ and $p_{occipital} = 0.031$; Dataset 2: $Z_{frontal} = 2.044$ and $p_{frontal} = 0.041$, $Z_{central} = -2.082$ and $p_{central} = 0.041$). These ERPs were able to confirm the well-known findings (Javitt 2009; Javitt and Freedman 2015; Javitt et al. 2018) of impaired early response to external stimuli/tasks in SCZ participants.

We focused our subsequent analyses on the frontal electrodes because of previous studies (Egan et al. 2001; Weinberger et al. 2001; Winterer and Weinberger 2004; Rolls et al. 2008; Csukly et al. 2014; Weele et al. 2019) and our theta-centered hypothesis; our use of the surface Laplacian reference (Carvalhaes and De Barros 2015; Cohen 2015) meant that EEG activity in these frontal electrodes provided information on activity localized beneath these electrodes in the frontal cortex, more so than if the average reference was used.

We next calculated the SNR in a 200-ms sliding window as it measures the power of the signal relative to the background activity (noise) over time. The time interval of interest was just after stimulus onset (early in the trials) to capture the rapid change in neural activity due to stimulus onset.

Lower AUC in the SNR curves of specific frequency bands (broadband, theta, alpha) was found for the SCZ participants (Dataset 1: $Z_{broadband} = 2.932$ and $p_{broadband} = 0.005$, $Z_{theta} = 3.642$ and $p_{theta} < 0.001$, $Z_{alpha} = 2.028$ and $p_{alpha} = 0.043$; Dataset 2: $Z_{broadband} = 2.088$ and $p_{broadband} = 0.045$, $Z_{theta} = 2.107$ and $p_{theta} = 0.045$, $Z_{alpha} = 2.301$ and $p_{alpha} = 0.037$) (Fig. 1*b*). In Dataset 2, there was also a significantly lower AUC for SCZ participants in the gamma band ($Z_{gamma} = 2.007$, $p_{gamma} = 0.045$). This difference was not found in any of the other bands (Dataset 1: $p_{low\ beta} = 0.358$, $p_{high\ beta} = 0.663$, $p_{gamma} = 0.784$; Dataset 2: $p_{low\ beta} = 0.727$, $p_{high\ beta} = 0.262$) or in the later time interval (Supplementary Fig. 3).

When we plotted the mean SNR curves of all participants for each group (Supplementary Fig. 4 upper plot), we noticed clear peaks and troughs in the healthy control group. These were far less clear in the SCZ participants. To look more closely at this, we plotted the SNR curves for each participant in both groups to determine if the synchrony between curves differed within a group (Supplementary Fig. 4 lower plot). We hypothesized that the reason for the more flat mean curve in the SCZ group was due to differences in timing in SNR curves between participants; this would lead to a flatter curve when the mean of all participants was computed.

Therefore, to search for differences in the dynamic course, we calculated cross-correlation of SNR between participants in each group. This delay analysis, or synchrony between participants within each group, was quantified by cross-correlating the SNR curve for each participant with all other participants in their group (see Methods for details and Fig. 2*a*). This was only done for the theta and alpha bands as these were the bands in which significant differences were found in the SNR AUC. We hypothesized that there would be longer delays, therefore less synchrony, between participants in the SCZ group when compared with healthy controls.

Our statistical analysis comparing the delays between both groups in each dataset provides evidence to support this hypothesis. We found significantly longer delays between the SCZ participants in the theta and alpha bands in both datasets (Dataset 1: $Z_{theta} = -3.273$ and $p_{theta} = 0.002$, $Z_{alpha} = -2.017$ and $p_{alpha} = 0.044$; Dataset 2: $Z_{theta} = -2.271$ and $p_{theta} = 0.046$, $Z_{alpha} = -1.987$ and $p_{alpha} = 0.047$) (Fig. 2*b*). The SCZ participants, therefore, showed less synchrony with the other patients in their SNR curves in these two bands; the SNR curves of SCZ participants were less aligned than those of the healthy controls. The SCZ participants had lower interindividual temporal precision—higher variability—than the healthy controls.

The SNR delay finding which relates to timing between participants (within a group) led us to hypothesize that there was a difference between groups in phase synchronization within each individual participant to the stimulus at onset. This would require measuring

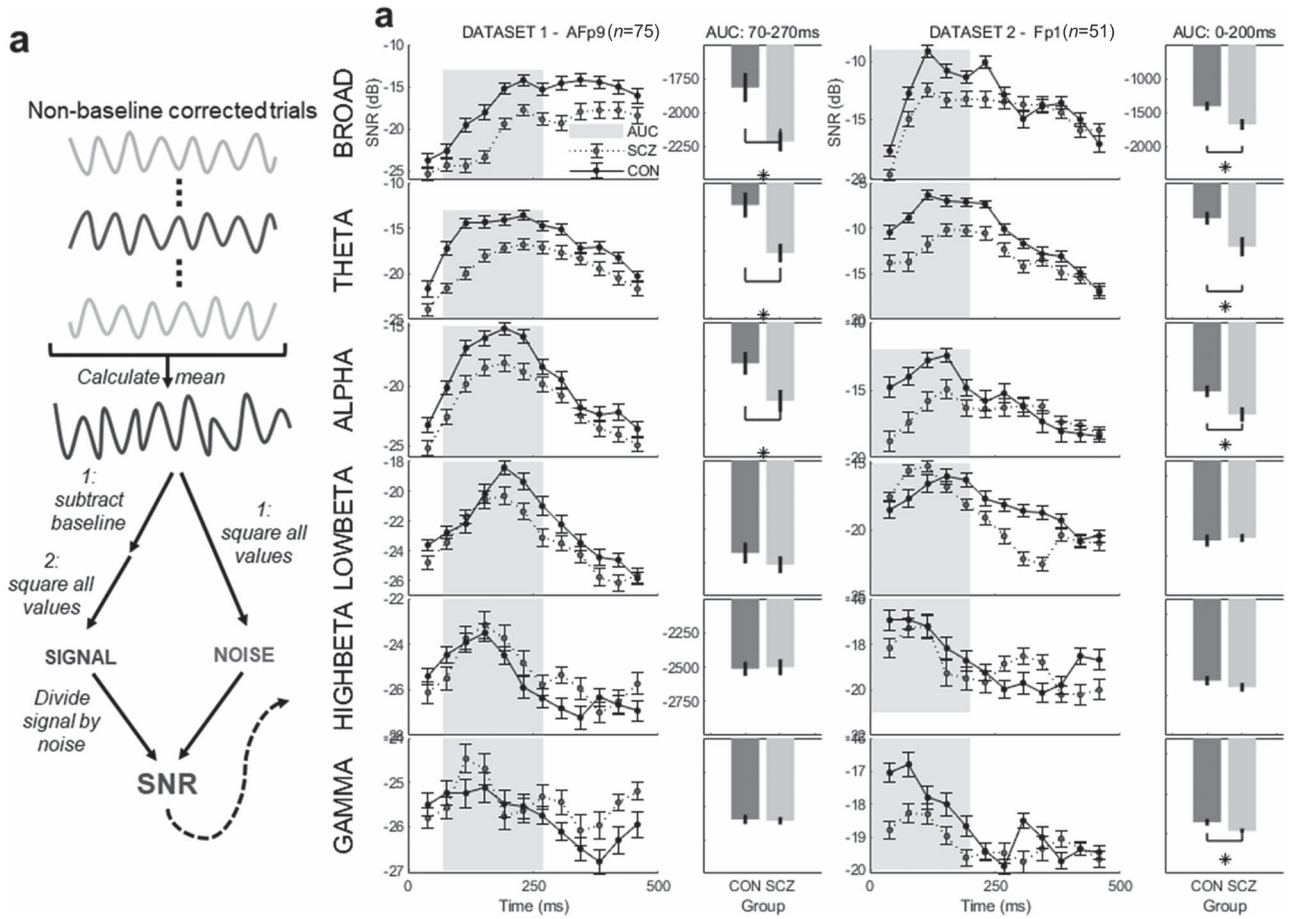

Figure 1. SNR in all frequency bands. (*a*) Calculation of SNR according to the methods of Xia (1998). The mean of all non-baseline corrected trials was first calculated between stimulus onset (0 ms) and 500 ms. To calculate the signal, the mean of the baseline interval (400 ms before stimulus onset to stimulus onset) was first subtracted from each timepoint, then each timepoint was squared. To calculate the noise, each timepoint was squared. The signal was then divided by the noise at each timepoint and was multiplied by 10 $\log_{10}$ to convert the units to decibels (dB). (*b*) SNR was calculated in a sliding window (length = 76 ms, overlap = 50%) for the broadband and each individual frequency band (broadband = 1–80 Hz; theta = 4–8 Hz; alpha = 8–13 Hz; low beta = 13–20 Hz; high beta = 20–30 Hz; gamma = 30–80 Hz.). An early time interval was chosen (Dataset 1 = 70–270 ms; Dataset 2 = 0–200 ms; gray patch) and the AUC was calculated and statistically tested (bar plots). The AUC was significantly lower in SCZ in the broadband and in theta and alpha in both datasets. In Dataset 2, the SNR AUC in SCZ was lower in the gamma band also. All *P* values are corrected for multiple comparisons using Benjamini–Hochberg false discovery rate (FDR).

temporal precision over trials within each participant and comparing the two groups. To measure this, we calculated ITPC. ITPC measures the phase angle coherence over all trials at each time point and frequency, so the consistency over trials. In contrast to the delay analysis, this measure looks at timing within each participant over all their trials. From our results showing less synchrony between SCZ participants, so lower interindividual temporal precision, we hypothesized that SCZ participants would have lower ITPC, so lower intraindividual temporal precision soon after stimulus onset, especially in the lower frequency bands.

Our ITPC results support this hypothesis. We found significantly lower phase coherence in the theta band just after stimulus onset (0–122 ms) in both datasets (Dataset 1: $Z_{theta} = 3.287$ and $p_{theta} = 0.003$; Dataset 2: $Z_{theta} = 2.384$ and $p_{theta} = 0.017$) (Fig. 3*a–c*). In Dataset 1, we also found significantly lower phase coherence in the delta band early in the trial in SCZ participants ($Z_{delta} = 2.749$ and $p_{delta} = 0.009$).

Therefore, our analyses found lower SNR in the broadband, theta, and alpha bands in the early time interval. We also found 1) lower interindividual temporal precision in the SCZ group—higher delays between SCZ participants—in the theta and alpha bands; 2) lower intraindividual temporal precision in the SCZ participants—lower consistency in phase over trials in each SCZ participant—also in the theta and alpha bands (delta was omitted as the time windows allowed for too few datapoints in this frequency band with long cycles). These findings were consistent in both datasets.

ITPC Computational Simulations Reveal Temporally Imprecise Phase Shifting in SCZ

After our above results, we posited that this difference in delays and ITPC was due to more irregular phase shifting in the SCZ participants. This would lead to differences in temporal precision (consistency, or the inverse of variance) with respect to the stimulus and likely lead to

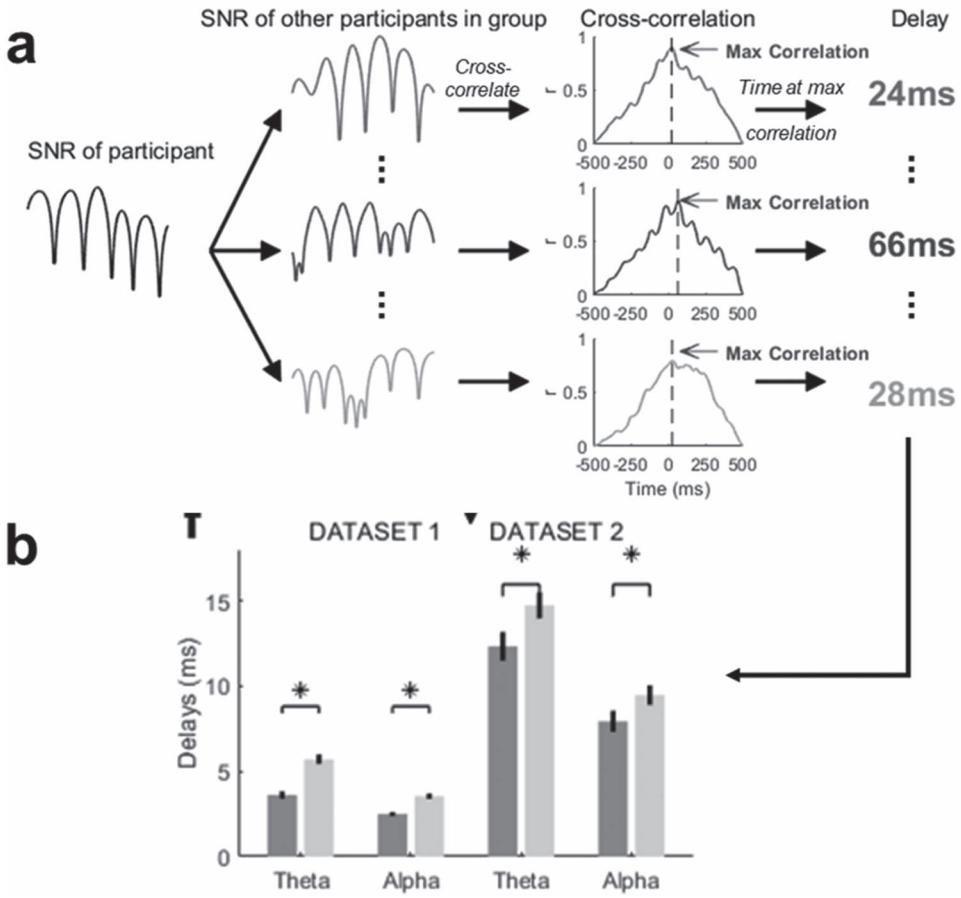

Figure 2. SNR cross-correlation delay analysis in theta and alpha bands. (*a*) We did a cross-correlation of the SNR curve in the theta and alpha bands for each participant with all other participants in their group. For example, participant 1 in the SCZ group had their theta and alpha SNR signals cross-correlated with that of participants 2, 3, 4, etc. of the SCZ group. The time at maximum cross-correlation (time at black dashed lines) was determined. The absolute value of this time (in ms) then constituted the time delay between the two SNR signals being cross-correlated: For example, a delay of 7 ms between participants 1 and 2 of the SCZ group. (*b*) Time delays between groups were statistically compared. The time delays in the CON group were found to be significantly shorter than those in the SCZ group in both bands and both datasets. All *P*-values are corrected for multiple comparisons using Benjamini–Hochberg FDR.

lower SNR in the early time interval. The SCZ participants would have irregular phase shifting in each trial, so over trials this would result in lower phase consistency within each participant, and higher delays between participants.

To demonstrate this relationship between delays and phase shifting with ITPC directly, we decided to do computational simulations which only varied the degree of phase shifting. We would simulate a set of data with multiple trials in which there was no phase shifting (negative control), a set with complete phase shifting (positive control), and three sets between the two. From these simulated datasets—in which the "ground truth," or known properties, of the sine waves would be known—the ITPC would be measured using the same methods as shown previously. The results of the simulations would then be compared with our actual results. This link to the actual results would allow us to infer the amount of phase shifting in each of the groups, thus quantifying the phase shifting differences between the SCZ participants and the healthy controls.

To model our simulations as close as possible on our actual data, we looked at the event-related spectral perturbation (ERSP) of our actual data (Supplementary Figs 5*a* and 7). In both groups of both datasets, the common ERSP results showed a poststimulus increase in theta power (also supported by theta findings in SCZ; Başar and Güntekin 2013; Csukly et al. 2014) after stimulus onset. There were other changes in power seen (beta, high delta increase in Dataset 1; high delta increase in Dataset 2), but these varied between the two datasets. Consequently, this brief increase in theta power is the basis for the sine waves in our simulations (see Materials and Methods for details). Therefore, the simulations were as close to the actual data as possible.

When inspecting the simulations, the poststimulus ITPC in the theta band is highest with no phase shift (far left plot) and decreases in the plots to the right. As expected, the lowest ITPC was in the far right plot which had a phase shift of 2π. These results were consistent in Datasets 1 and 2, regardless of the number of trials, though the level of ITPC does vary. Next, from the actual ITPC data (Fig. 4*c*), the ITPC for each participant at stimulus onset at 6 Hz was calculated (Fig. 4*d*). From this ITPC at 6 Hz, the Euclidean distance (*d*) to the ITPC values at stimulus onset and 6 Hz for each simulation

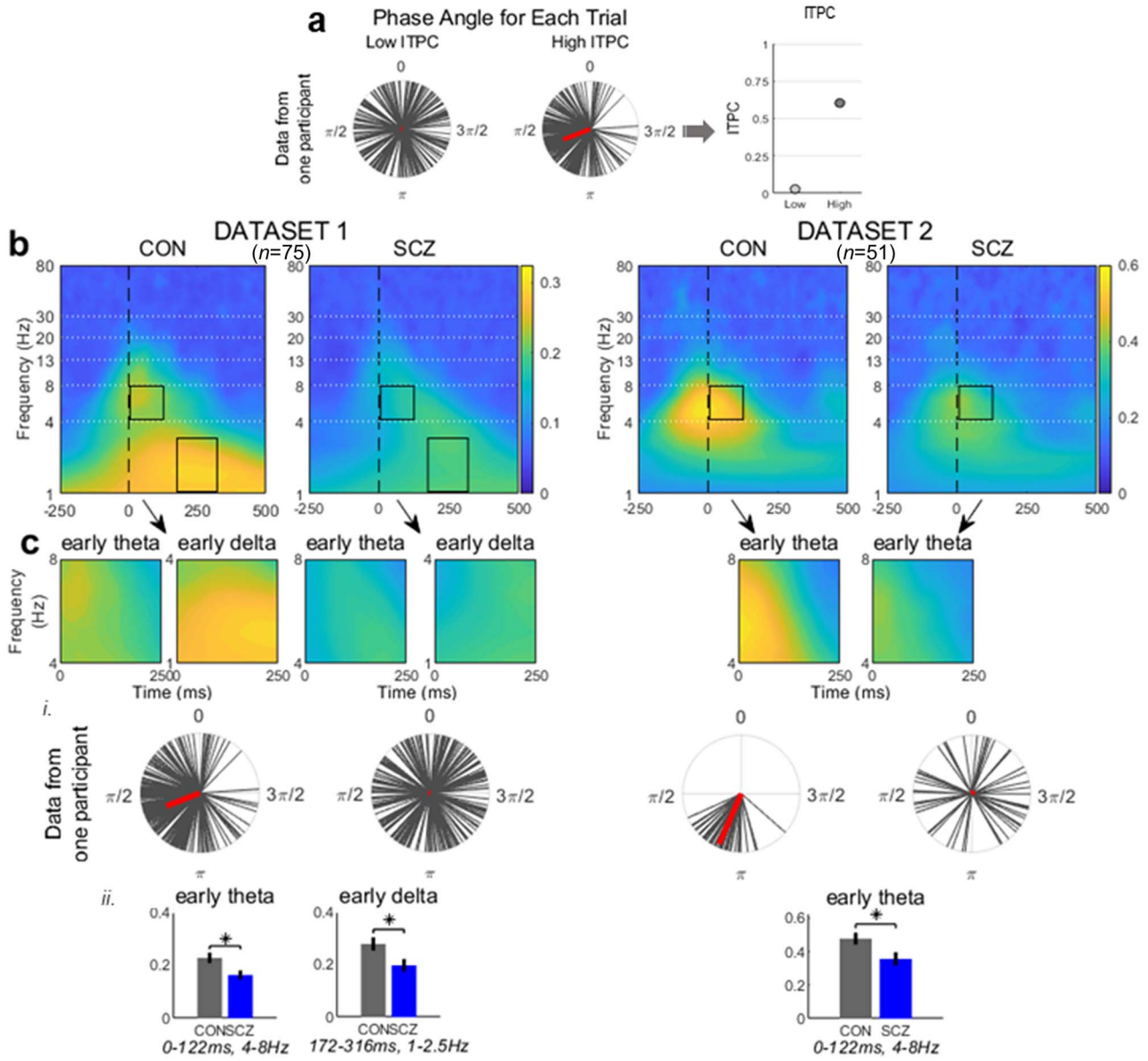

Figure 3. ITPC in SCZ. (*a*) ITPC is calculated based on the phase angle at a specific timepoint and frequency (here shown as 6 Hz at stimulus onset or 0 ms) for all trials. The dark gray lines in the polar phase plot represent the phase angle for each trial (216 trials so 216 phase angles). In low ITPC (left), there is no preferred phase, so the distribution of phase angle is uniform, or spread evenly around the circle. In contrast, in high ITPC (right), there is a greater proportion of the phase angles in one part of the circle and not phase angles at another part; the distribution is nonuniform so not evenly spaced around the circle. The red bar (difficult to see in the low ITPC case) signifies the ITPC resulting from the individual gray lines. The longer the red bar, the higher the ITPC (shown at right scatter plot), with a maximum of 1. (*b*) ITPC in both datasets for the first 500 ms after stimulus onset. After visualizing the contour plots, data from two areas in Dataset 1 (theta and delta bands) and one area in Dataset 2 (theta band) (*c*) were extracted (black rectangles). (i) Polar histograms (each bin = 20°) measuring percent of participants preferred (mean) phase angle at 6 Hz and stimulus onset in bins. For example, if the top of a bar touches the 20% radius, then 20% of the participants in that group have a preferred phase angle in that bin. (ii) The data extracted in a/b were statistically compared, with lower phase coherence found in the SCZ participants in both datasets.

was measured. The lowest of these, thus the smallest Euclidean distance, indicated the phase shift closest to the actual data.

In Dataset 1, this was a phase shift of $^{3\pi}/_{2}$ ($d = 0.928$) for the healthy controls and 2π ($d = 0.869$) for the SCZ participants (see Supplementary Table 3 for the other Euclidean distances). In Dataset 2, this was a phase shift of $^{\pi}/_{2}$ ($d = 0.972$) for the healthy controls and π ($d = 1.187$) for the SCZ participants.

This showed that the simulation closest to the actual data had greater phase shifting, so lower ITPC, in the SCZ groups of both datasets. Therefore, the simulations were able to demonstrate and link the actual data to phase shifting. They were able to illustrate that there was more irregular phase shifting in the SCZ groups than in the CON groups.

SNR and ITPC Correlate Significantly but Do Not Predict Reaction Times in SCZ and Are Lower in Slow and Fast Trials in SCZ

Next, we determined the relationship between SNR and ITPC. To link the two measures, we correlated theta phase

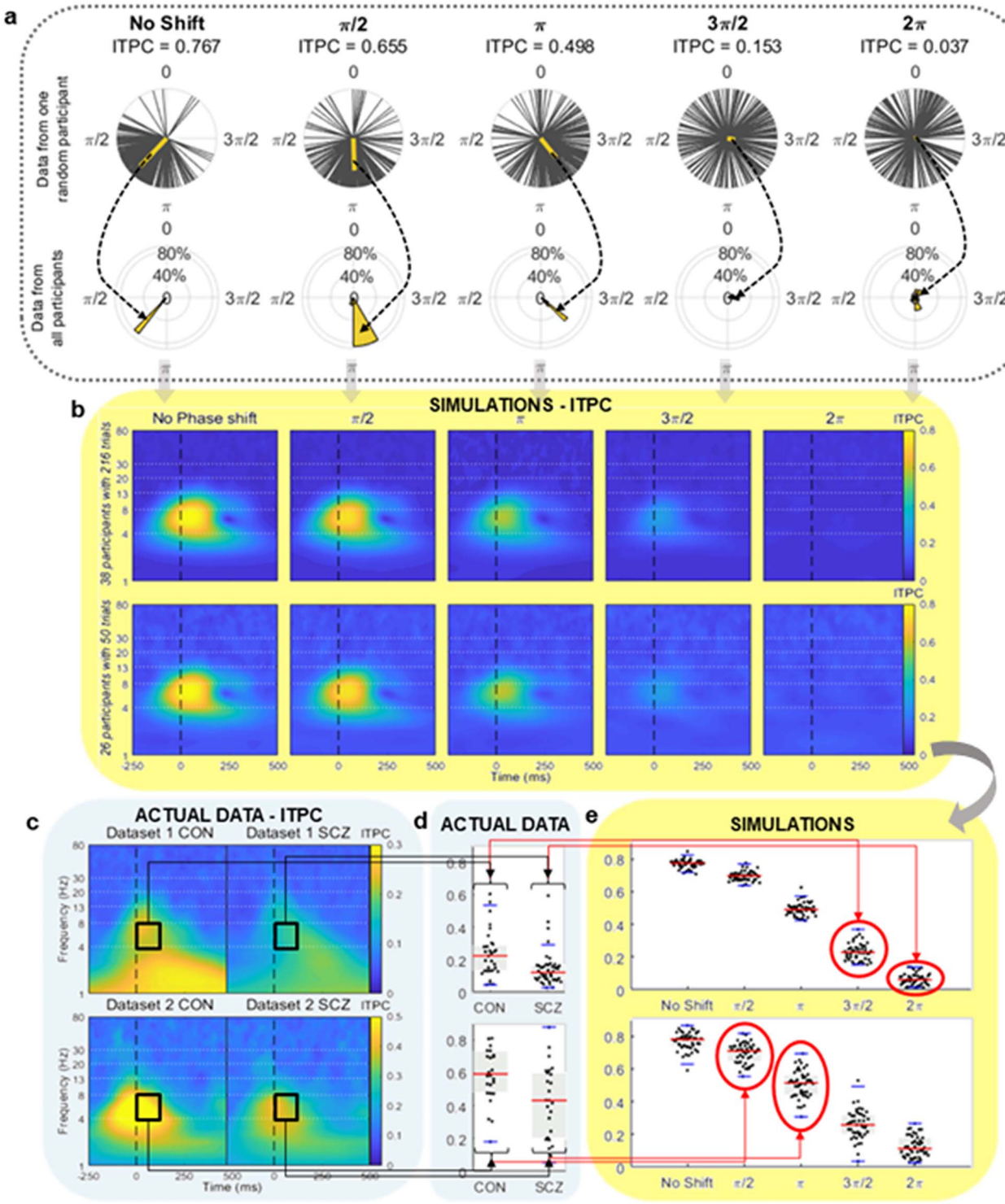

Figure 4. Simulation of ITPC with five levels of phase shifting. (*a*) The phase shifts described in the middle right plot of (*b*) have direct effects on the phase coherence over trials, which is what ITPC measures. In the top row, one participant in the simulation was randomly chosen to visualize the phase angle at stimulus onset at 6 Hz for each level of phase shift. The dark gray lines in each polar plot represent that phase angle for one trial; there are 216 trials, so 216 gray lines. The thick yellow line is the preferred phase angle resulting from all the trials and the ITPC; the longer the line, the more consistent the phase angle over all trials and the higher the ITPC. The far left plot ('No Phase shift') has no phase shift, therefore the highest ITPC and longest thick yellow line. This decreases across the plots to the far right plot with the lowest ITPC and shortest thick yellow line. As the ITPC decreases, the phase angles for all trials become more uniform and spread out around the circle in the polar plot. In the second row, each polar plot contains data from all participants and is a histogram which measures the percentage of participants whose preferred phase angle falls within that bin. When a bin touches the 80% radial line, then the preferred phase angles of 80% of the participants occurred at that phase angle. This occurs in the far left plot; bars become shorter and more numerous, so the preferred phases become more spread around the circle, in the more right plots. (*b*) The resulting ITPC plots of the simulations. The first row constitutes 38 participants (mean of 31 CON and 44 SCZ) of one channel each and 216 trials, the same parameters of Dataset 1. The second row constitutes 26 participants with one channel each and 50 trials, which are the same parameters of Dataset 2. The poststimulus ITPC in the theta band is highest in the far left plot (no phase shift) and decreases in the plots to the right, with the lowest in the far right plot which has a phase shift of 2π. (*c*) Actual ITPC data from both datasets (top row: Dataset 1; bottom row: Dataset 2). The preferred phase angle and ITPC

coherence after stimulus onset with SNR AUC using Spearman correlation, and fit linear curves (Fig. 5*a*). This was done only in the bands where we found significant differences in SNR AUC, so in broadband, theta, and alpha (hereafter termed "relevant bands").

We found significant correlations and fits in all relevant bands in both datasets (Dataset 1: $\rho_{broadband} = 0.681$, $p_{broadband} < 0.001$, $R^2 = 0.464$; $\rho_{theta} = 0.512$, $p_{theta} < 0.001$, $R^2 = 0.262$; $\rho_{alpha} = 0.481$, $p_{alpha} < 0.001$, $R^2 = 0.231$; Dataset 2: $\rho_{broadband} = 0.803$, $p_{broadband} < 0.001$, $R^2 = 0.645$; $\rho_{theta} = 0.860$, $p_{theta} < 0.001$, $R^2 = 0.740$; $\rho_{alpha} = 0.536$, $p_{alpha} < 0.001$, $R^2 = 0.287$).

Finally, our last question concerned the behavioral relevance of SNR: Is there a difference in SNR and early phase coherence between groups in fast and slow trials? To answer this question, we computed SNR curves for both groups in the fastest and slowest 40% of trials ($p_{fast\ RT} = 0.119$, $p_{slow\ RT} = 0.028$) (Fig. 5*b*). This was only done in Dataset 1 as Dataset 2 was a no-report paradigm (Tsuchiya et al. 2015) and therefore had no responses and reaction times.

We found lower SNR AUC in SCZ participants in both the fast and slow trials, as well as lower ITPC and decreased difference between fast and slow trials. In the fast trials of Dataset 1, SCZ participants had lower SNR AUC and early phase coherence than healthy controls ($Z_{SNR} = 1.985$, $p_{SNR} = 0.047$; $Z_{ITPC} = 2.265$, $p_{ITPC} = 0.047$) (Fig. 5*c*–*f*). This same finding was seen in the slow trials ($Z_{SNR} = 2.168$, $p_{SNR} = 0.047$; $Z_{ITPC} = 1.972$, $p_{ITPC} = 0.049$). When the difference in phase coherence between fast and slow trials was calculated for each group (fast—slow), we found a significantly smaller difference in the SCZ participants than the healthy controls ($Z = 2.027$, $p = 0.049$) (Fig. 5*g*). These results show that SCZ participants had less difference between fast and slow trials in early phase coherence compared with healthy controls.

Finally, to determine if the linear relationship between two predictors (ITPC AUC and SNR AUC) and the response variable (mean reaction time) differed between experimental groups, a multiple linear regression was done for each group independently (Fig. 5*h*,*i*). In the healthy controls, a significant regression equation was found ($F(2,90) = 6.21$, $P = 0.003$) with an R^2 of 0.121. Thus, the predicted mean reaction time of a healthy participant is equal to 0.484 s – 0.003 s (ITPC AUC) + 0.012 s (SNR AUC), where ITPC AUC is measured in coherence·ms and SNR AUC is measured in dB·ms. Of note, SNR is measured in decibels (dB), which are negative in our results (see Fig. 1). Both ITPC ($\beta = -0.003$, $P = 0.009$) and SNR AUC ($\beta = 0.012$, $P = 0.014$) were significant predictors of mean reaction time in healthy participants.

In contrast, no significant regression equation in the SCZ participants was found ($F(2,129) = 1.76$, $P = 0.177$) with an R^2 of 0.027. Neither ITPC ($\beta = -0.002$, $P = 0.097$) nor SNR AUC ($\beta = -0.002$, $p = 0.616$) were significant predictors of mean reaction time in SCZ participants.

Therefore, our results suggest that 1) the greater the theta phase coherence just after stimulus onset, the larger the SNR AUC in the early interval in the relevant bands; 2) SNR and ITPC are behaviorally relevant; and 3) ITPC and SNR AUC predict reaction time in healthy controls but not in SCZ participants.

Discussion

Findings on sensory perception (Javitt 2009; Sass et al. 2013; Vlcek et al. 2014; Javitt and Freedman 2015; Micoulaud-Franchi et al. 2016; Hoptman et al. 2018) and cognition (Schwartz et al. 1989; Birkett et al. 2007) in SCZ suggest that the brain's neuronal background activity (Winterer and Weinberger 2004) intermittently overwhelms the processing of external stimuli (Yang et al. 2014, 2017). This impedes consistency and temporal precision in external stimulus processing (Andreasen et al. 1999; Thoenes and Oberfeld 2017), which manifests in increased variability in behavioral responses and ultimately in deficits in cognition and behavior.

Building on previous results in static SNR (Winterer et al. 1999; Winterer and Weinberger 2004), our first main finding extends these by 1) showing group differences in SNR in two different SCZ datasets with different sensory modalities and experimental paradigms; 2) isolating differences in SNR to the early time interval just after stimulus onset; 3) isolating SNR differences to the broadband, theta, and alpha bands. In addition, our SNR cross-correlation analysis found significantly longer delays, therefore less synchrony, between participants in the SCZ group in the theta and alpha bands. Again, this was found in both SCZ datasets.

Lower theta ITPC in SCZ participants is our second main finding. From our SNR results and the lower synchrony between the SNR curves in the SCZ group as measured through delays, we hypothesized that lower phase coherence over trials was likely in these patients, as was found in a previous study (Lakatos et al. 2013). Our ITPC results support this hypothesis, and our computational simulations show that higher phase shifting leads to lower ITPC. Lower phase coherence over trials fits with the rhythmic versus continuous mode results and hypothesis of Lakatos et al. (2013), and the impaired precision (higher variability over trials) found in SCZ participants related to timing (Thoenes and Oberfeld 2017).

for each participant at stimulus onset at 6 Hz were calculated in the actual data. (*d*) The Euclidean distance between the calculated ITPC values and the ITPC values in each of the simulations was measured. (*e*) The ITPC of the phase shift simulation which was closest to the actual ITPC data was determined as that of the lowest Euclidean distance, so the closest. This showed that the simulation closest to the actual data had greater phase shifting, so lower ITPC, in the SCZ groups of both datasets. Therefore, the simulations were able to link the actual data to phase shifting, showing that there was greater phase shifting in the SCZ groups than in the CON groups. Blue rectangles = actual data; yellow rectangles = simulations; gray dashed rectangles = methods.

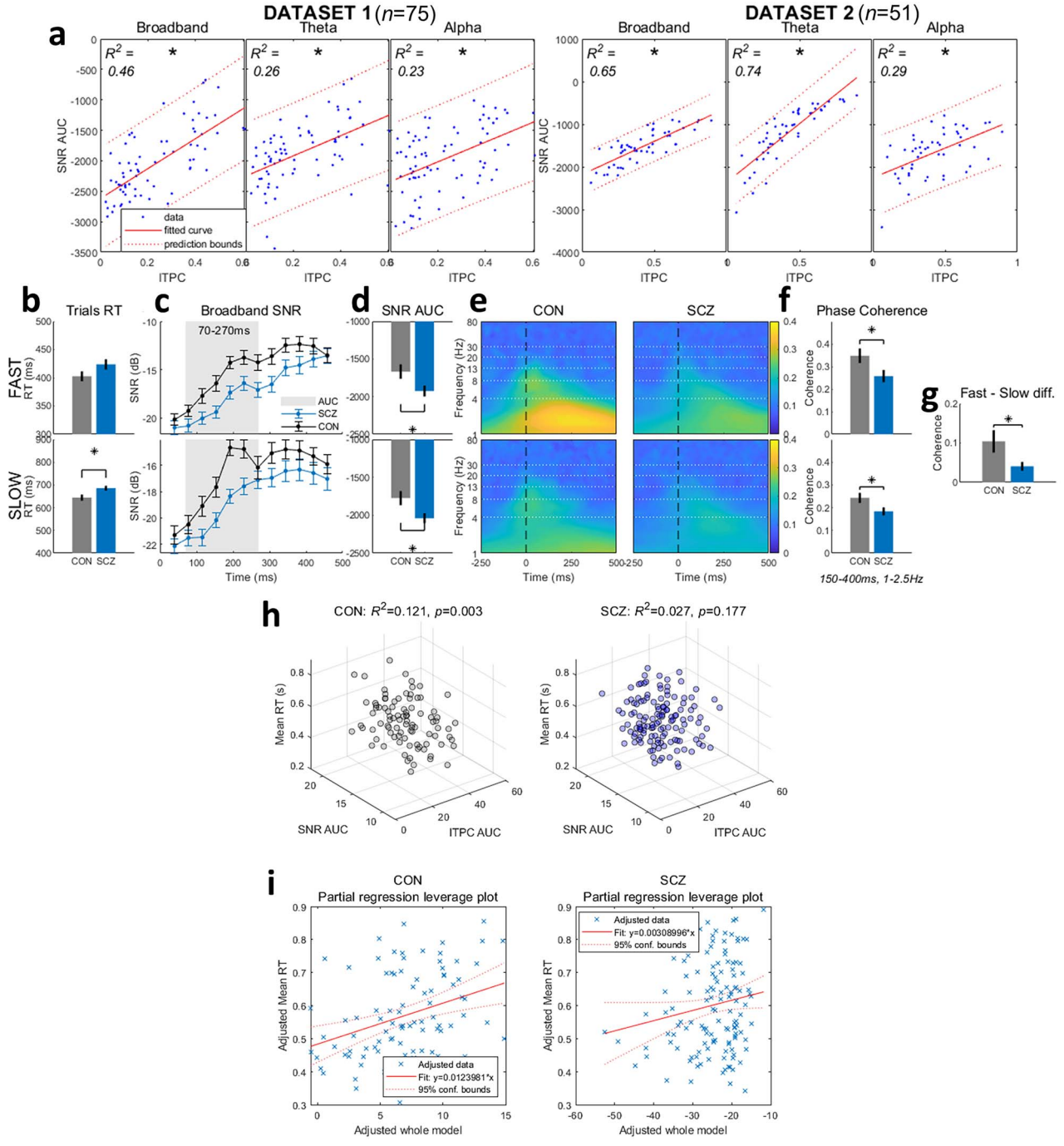

Figure 5. ITPC and SNR correlation and their behavioral relevance. (*a*) Linear model fits (polynomial = 1) between ITPC and SNR AUC in both datasets for the frequency bands found to be significant in the earlier analysis (broadband, theta, alpha). The Spearman correlations were all significant (R^2 values in plots). (*b*) Difference in mean reaction times for the fastest and slowest 40% of trials between the SCZ and CON groups. (*c*) From the fastest and slowest 40% of trials, the SNR in a sliding window was calculated. (*d*) The SNR AUC was significantly lower in the SCZ group for both the fast and slow trials. (*e*) ITPC of fast and slow trials for each group. (*f*) Extracted ITPC values between 1–2.5 Hz and 150–400 ms after stimulus onset. In both fast and slow trials, SCZ participants had significantly lower ITPC than the healthy controls. (*g*) When the difference between the ITPC in the fast and slow trials was calculated (fast – slow), there was less of a difference in the SCZ participants than the healthy controls. (*h*) All trials were divided into three groups according to reaction times (slow, middle, fast), and SNR and ITPC were calculated in the corresponding EEG data. Results were then extracted for each participant in both SNR (0–200 ms) and ITPC (0–200 ms, 1–8 Hz) for each reaction time group (3 groups). In a multiple linear regression model for each experimental group, both SNR AUC and ITPC AUC were significant predictors of mean reaction time in the healthy controls (CON, left plot, black markers). This was not the case in the SCZ participants (right plot, blue markers). (*i*) Partial regression leverage plots for each multiple linear regression model.

For the first time, we were able to link the decreased ITPC in SCZ participants to decreased SNR as we showed through correlations and linear fits.

Together, our findings strongly support our overarching expectation, namely that SCZ participants show temporal imprecision on the neural level, and how it mediates temporal imprecision on the behavioral level. If found to be specific to SCZ, this creates the possibility that, if confirmed in larger cohorts, temporal imprecision of SNR and ITPC may serve as biomarker for SCZ and subsequently be used clinically in differential diagnosis of SCZ.

When considering our above described results, several important limitations must be considered. Firstly, we investigated SNR only—not its components, signal and noise—and only one variation (Xia 1998) of the measure. A second, slightly different method of measuring SNR (Winterer et al. 1999), and its decomposition into the two components (Winterer et al. 2004), should be done in a future study to delve further into the specifics of differences in SNR related to SCZ. Our findings of differences in SNR in the SCZ group could be due to differences in signal, noise, or both and must be investigated further. In addition, our method of SNR calculation (Xia 1998) considered evoked activity as signal; however, considering evoked and induced activity (David et al. 2006) as signal should be investigated in a future study. Next, participants in the experimental groups were all medicated, thus having a confounding factor that was accounted for by co-variation. Unfortunately, we were limited in this by the availability of appropriate datasets and the impossibility of clinical patients without medications; a future study in a large-scale dataset, preferably with some nonmedicated experimental group participants, should be done to verify our results found here.

Next, the experimental paradigm in Dataset 1, the Cost Conflict task, is a complex cognitive task. For this reason, our findings could be confounded by various factors, including the cognitive demand of the task itself. We mitigated for this by analyzing only the first 500 ms of each trial even though participants had 850 ms to respond to the stimuli. Furthermore, the possibility of our results being due to the cognitive demands of the task is undermined by our replication of results in Dataset 2, which had a simple auditory stimulus without response.

The third limitation relates to methodological considerations for ITPC. ITPC is more likely to show results in lower frequencies than in higher frequencies as the phase cycles are longer in lower frequencies. Therefore, this analysis may have failed to detect true ITPC in higher frequencies, in addition to our findings in theta and delta.

Conclusion

Our general aim of this study was to investigate temporal imprecision in SCZ on the neural level and link it to temporal imprecision in behavior. We show reduction in the dynamics, that is, temporal synchronization of two neural measures, namely SNR and ITPC, which hold across different task states in SCZ. Reductions in both SNR and ITPC relate to each other (as presumably based on the shared temporal imprecision) and mediate timing on the behavioral level, namely slow and fast reaction times. Together, our findings strongly support that SCZ is characterized by diagnosis-specific temporal imprecision on the neural level and its relation to corresponding temporal imprecision on the behavioral level. Our findings provide evidence for the use of temporal imprecision in SNR and ITPC serving as potential biomarker.

Supplementary Material

Supplementary material can be found at *Cerebral Cortex* online.

Funding

EJLB-Michael Smith Foundation; Canadian Institutes of Health Research; Ministry of Science and Technology of China; National Key R&D Program of China (2016YFC1306700); Hope of Depression Foundation (HDRF); Start-Up Research Grant in Hangzhou Normal University (to G.N.); European Union's Horizon 2020 Framework Program for Research and Innovation under the Specific Grant Agreement No. 785907 (Human Brain Project SGA2).

Notes

Conflict of Interest: The authors declare no known conflicts of interest.

References

Abi-Dargham A. 2020. From "bedside" to "bench" and back: a translational approach to studying dopamine dysfunction in schizophrenia. *Neurosci Biobehav Rev.* 110:174–179.

Aghababaiyan K. 2020. Improving performance of neurons by adding colour noise. *IET Nanobiotechnol.* 14:433–439.

Albrecht MA, Waltz JA, Cavanagh JF, Frank MJ, Gold JM. 2019. Increased conflict-induced slowing, but no differences in conflict-induced positive or negative prediction error learning in patients with schizophrenia. *Neuropsychologia.* 123:131–140.

Andreasen NC, Nopoulos P, O'Leary DS, Miller DD, Wassink T, Flaum M. 1999. Defining the phenotype of schizophrenia: cognitive dysmetria and its neural mechanisms. *Biol Psychiatry.* 46:908–920.

Andreasen NC, Pierson R. 2008. The role of the cerebellum in schizophrenia. *Biol Psychiatry.* 64:81–88.

Arazi A, Censor N, Dinstein I. 2017. Neural variability quenching predicts individual perceptual abilities. *J Neurosci.* 37:97–109.

Baker DH, Richard B. 2019. Dynamic properties of internal noise probed by modulating binocular rivalry. *PLoS Comput Biol.* 15:1–18.

Başar E, Güntekin B. 2013. Review of delta, theta, alpha, beta, and gamma response oscillations in neuropsychiatric disorders. *Suppl Clin Neurophysiol.* 62:303–341.

Benjamini Y, Hochberg Y. 1995. Controlling the false discovery rate : a practical and powerful approach to multiple testing. *J R Stat Soc.* 57:289–300.

Berry SD, Thompson RF. 1978. Prediction of learning rate from the hippocampal electroencephalogram. *Science (80-)*. 200:1298–1300.
Bigdely-Shamlo N, Mullen T, Kothe C, Su KM, Robbins KA. 2015. The PREP pipeline: standardized preprocessing for large-scale EEG analysis. *Front Neuroinform*. 9:1–19.
Birkett P, Sigmundsson T, Sharma T, Toulopoulou T, Griffiths TD, Reveley A, Murray R. 2007. Reaction time and sustained attention in schizophrenia and its genetic predisposition. *Schizophr Res*. 95: 76–85.
Bolbecker AR, Westfall DR, Howell JM, Lackner RJ, Carroll CA, O'Donnell BF, Hetrick WP. 2014. Increased timing variability in schizophrenia and bipolar disorder. *PLoS One*. 9:1–8.
Carvalhaes C, De Barros JA. 2015. The surface Laplacian technique in EEG: theory and methods. *Int J Psychophysiol*. 97:174–188.
Choueiry J, Blais CM, Shah D, Smith D, Fisher D, Labelle A, Knott V. 2019. Combining CDP-choline and galantamine, an optimized $\alpha 7$ nicotinic strategy, to ameliorate sensory gating to speech stimuli in schizophrenia. *Int J Psychophysiol*. 145:70–82.
Cohen MX. 2015. Comparison of different spatial transformations applied to EEG data: a case study of error processing. *Int J Psychophysiol*. 97:245–257.
Csukly G, Stefanics G, Komlósi S, Czigler I, Czobor P. 2014. Event-related theta synchronization predicts deficit in facial affect recognition in schizophrenia. *J Abnorm Psychol*. 123:178–189.
David O, Kilner JM, Friston KJ. 2006. Mechanisms of evoked and induced responses in MEG/EEG. *Neuroimage*. 31:1580–1591.
Delorme A, Makeig S. 2004. EEGLAB: an open source toolbox for analysis of single-trial EEG dynamics. *J Neurosci Methods*. 134:9–21.
Egan MF, Goldberg TE, Kolachana BS, Callicott JH, Mazzanti CM, Straub RE, Goldman D, Weinberger DR. 2001. Effect of COMT Val108/158 Met genotype on frontal lobe function and risk for schizophrenia. *Proc Natl Acad Sci U S A*. 98:6917–6922.
Einevoll GT, Destexhe A, Diesmann M, Grün S, Jirsa V, de Kamps M, Migliore M, Ness TV, Plesser HE, Schürmann F. 2019. The scientific case for brain simulations. *Neuron*. 102:735–744.
Fan X, Markram H. 2019. A brief history of simulation neuroscience. *Front Neuroinform*. 13:1–28.
Frankle WG, Narendran R. 2020. Distinguishing schizophrenia subtypes: can dopamine imaging improve the signal-to-noise ratio? *Biol Psychiatry*. 87:197–199.
Gomez-Pilar J, de Luis-García R, Lubeiro A, de Uribe N, Poza J, Núñez P, Ayuso M, Hornero R, Molina V. 2018. Deficits of entropy modulation in schizophrenia are predicted by functional connectivity strength in the theta band and structural clustering. *NeuroImage Clin*. 18:382–389.
Gray JA. 1982. The neuropsychology of anxiety: an enquiry into the functions of the septo-hippocampal system. *Behav Brain Sci*. 5: 469–484.
Guevara Erra R, Arbotto M, Schurger A. 2019. An integration-to-bound model of decision-making that accounts for the spectral properties of neural data. *Sci Rep*. 9:1–12.
Hafting T, Fyhn M, Bonnevie T, Moser M-B, Moser EI. 2008. Hippocampus-independent phase precession in entorhinal grid cells. *Nature*. 453:1248–1252.
Hamilton HK, Roach BJ, Cavus I, Teyler TJ, Clapp WC, Ford JM, Tarakci E, Krystal JH, Mathalon DH. 2020. Impaired potentiation of theta oscillations during a visual cortical plasticity paradigm in individuals with schizophrenia. *Front Psychiatry*. 11:1–14.
Hoptman MJ, Parker EM, Nair-Collins S, Dias EC, Ross ME, DiCostanzo JN, Sehatpour P, Javitt DC. 2018. Sensory and cross-network contributions to response inhibition in patients with schizophrenia. *NeuroImage Clin*. 18:31–39.
Javitt DC. 2009. Sensory processing in schizophrenia: neither simple nor intact. *Schizophr Bull*. 35:1059–1064.
Javitt DC, Freedman R. 2015. Sensory processing dysfunction in the personal experience and neuronal machinery of schizophrenia. *Am J Psychiatry*. 172:17–31.
Javitt DC, Lee M, Kantrowitz JT, Martinez A. 2018. Mismatch negativity as a biomarker of theta band oscillatory dysfunction in schizophrenia. *Schizophr Res*. 191:51–60.
Jurcak V, Tsuzuki D, Dan I. 2007. 10/20, 10/10, and 10/5 systems revisited: their validity as relative head-surface-based positioning systems. *Neuroimage*. 34:1600–1611.
Kesby JP, Eyles DW, McGrath JJ, Scott JG. 2018. Dopamine, psychosis and schizophrenia: the widening gap between basic and clinical neuroscience. *Transl Psychiatry*. 8:30.
Korotkova T, Ponomarenko A, Monaghan CK, Poulter SL, Cacucci F, Wills T, Hasselmo ME, Lever C. 2018. Reconciling the different faces of hippocampal theta: the role of theta oscillations in cognitive, emotional and innate behaviors. *Neurosci Biobehav Rev*. 85:65–80.
Lakatos P, Schroeder CE, Leitman DI, Javitt DC. 2013. Predictive suppression of cortical excitability and its deficit in schizophrenia. *J Neurosci*. 33:11692–11702.
Micoulaud-Franchi JA, Faugere M, Boyer L, Cermolacce M, Fond G, Richieri R, Vion-Dury J, Lancon C. 2016. Sensory gating deficits and impaired quality of life in patients with schizophrenia: a preliminary study. *Psychiatr Danub*. 28:225–233.
Mullen T. 2012. *NITRC: CleanLine: Tool/Resource Info*. https://www.nitrc.org/projects/cleanline/
Qu G, Fan B, Fu X, Yu Y. 2019. The impact of frequency scale on the response sensitivity and reliability of cortical neurons to $1/f\beta$ input signals. *Front Cell Neurosci*. 13:1–14.
Rentzsch J, Shen C, Jockers-Scherübl MC, Gallinat J, Neuhaus AH. 2015. Auditory mismatch negativity and repetition suppression deficits in schizophrenia explained by irregular computation of prediction error. *PLoS One*. 10:1–11.
Roach BJ, Ford JM, Loewy RL, Stuart BK, Mathalon DH. 2021. Theta phase synchrony is sensitive to corollary discharge abnormalities in early illness schizophrenia but not in the psychosis risk syndrome. *Schizophr Bull*. 47:415–423.
Rolls ET, Loh M, Deco G, Winterer G. 2008. Computational models of schizophrenia and dopamine modulation in the prefrontal cortex. *Nat Rev Neurosci*. 9:696–709.
Sass L, Pienkos E, Nelson B, Medford N. 2013. Anomalous self-experience in depersonalization and schizophrenia: a comparative investigation. *Conscious Cogn*. 22:430–441.
Schwartz F, Carr AC, Munich RL, Glauber S, Lesser B, Murray J. 1989. Reaction time impairment in schizophrenia and affective illness: the role of attention. *Biol Psychiatry*. 25:540–548.
Sterzer P, Adams RA, Fletcher P, Frith C, Lawrie SM, Muckli L, Petrovic P, Uhlhaas P, Voss M, Corlett PR. 2018. The predictive coding account of psychosis. *Biol Psychiatry*. 84: 634–643.
Thoenes S, Oberfeld D. 2017. Meta-analysis of time perception and temporal processing in schizophrenia: differential effects on precision and accuracy. *Clin Psychol Rev*. 54:44–64.
Tsuchiya N, Wilke M, Frässle S, Lamme VAF. 2015. No-report paradigms: extracting the true neural correlates of consciousness. *Trends Cogn Sci*. 19:757–770.
Van Diepen RM, Mazaheri A. 2018. The caveats of observing inter-trial phase-coherence in cognitive neuroscience. *Sci Rep*. 8:1–9.
Vlcek P, Bob P, Raboch J. 2014. Sensory disturbances, inhibitory deficits, and the P50 wave in schizophrenia. *Neuropsychiatr Dis Treat*. 10:1309–1315.

Weele CMV, Siciliano CA, Tye KM. 2019. Dopamine tunes prefrontal outputs to orchestrate aversive processing. *Brain Res*. 1713:16–31.

Weinberger DR, Egan MF, Bertolino A, Callicott JH, Mattay VS, Lipska BK, Berman KF, Goldberg TE. 2001. Prefrontal neurons and the genetics of schizophrenia. *Biol Psychiatry*. 50:825–844.

Winkler I, Brandl S, Horn F, Waldburger E, Allefeld C, Tangermann M. 2014. Robust artifactual independent component classification for BCI practitioners. *J Neural Eng*. 11:035013. https://doi.org/10.1088/1741-2560/11/3/035013.

Winkler I, Haufe S, Tangermann M. 2011. Automatic classification of Artifactual ICA- components for artifact removal in EEG signals. *Behav Brain Funct*. 7:30.

Winterer G, Egan MF, Raedler T, Sanchez C, Jones DW, Coppola R, Weinberger DR. 2004. Prefrontal broadband noise, working memory, and genetic risk for schizophrenia. *Am J Psychiatry*. 161: 490–500.

Winterer G, Weinberger DR. 2004. Genes, dopamine and cortical signal-to-noise ratio in schizophrenia. *Trends Neurosci*. 27:683–690.

Winterer G, Ziller M, Dorn H, Frick K, Mulert C, Dahhan N, Herrmann WM, Coppola R. 1999. Cortical activation, signal-to-noise ratio and stochastic resonance during information processing in man. *Clin Neurophysiol*. 110:1193–1203.

Winterer G, Ziller M, Dorn H, Frick K, Mulert C, Wuebben Y, Herrmann WM, Coppola R. 2000. Schizophrenia: reduced signal-to-noise ratio and impaired phase-locking during information processing. *Clin Neurophysiol*. 111:837–849.

Xia X. 1998. A quantitative analysis of SNR in the short-time Fourier transform domain for multicomponent signals. *IEEE Trans SIGNAL Process*. 46:200–203.

Yang GJ, Murray JD, Glasser M, Pearlson GD, Krystal JH, Schleifer C, Repovs G, Anticevic A. 2017. Altered global signal topography in schizophrenia. *Cereb Cortex*. 27:5156–5169.

Yang GJ, Murray JD, Repovs G, Cole MW, Savic A, Glasser MF, Pittenger C, Krystal JH, Wang X-J, Pearlson GD, et al. 2014. Altered global brain signal in schizophrenia. *Proc Natl Acad Sci U S A*. 111: 7438–7443.